Negative Thermal Expansion in Hybrid Improper Ferroelectric Ruddlesden-Popper Perovskites by Symmetry Trapping

M. S. Senn,[1,2,*] A. Bombardi,[1] C. A. Murray,[1] C. Vecchini,[3] A. Scherillo,[4] X. Luo,[5] and S. W. Cheong[5,6]
[1]Diamond Light Source Limited, Harwell Science and Innovation Campus, Didcot OX11 0DE, United Kingdom
[2]Department of Chemistry, Inorganic Chemistry Laboratory, University of Oxford, South Parks Road, Oxford OX1 3QR, United Kingdom
[3]National Physical Laboratory, Hampton Road, Teddington TW11 0LW, United Kingdom
[4]ISIS, STFC, Rutherford Appleton Laboratory, Didcot OX11 0QX, United Kingdom
[5]Laboratory for Pohang Emergent Materials and Department of Physics, Pohang University of Science and Technology, Pohang 790-784, Korea
[6]Rutgers Center for Emergent Materials and Department of Physics and Astronomy, Rutgers University, Piscataway, New Jersey 08854, USA
(Received 9 September 2014; published 22 January 2015)

We present new results on the microscopic nature of the ferroelectricity mechanisms in $Ca_3Mn_2O_7$ and $Ca_3Ti_2O_7$. To the first approximation, we confirm the hybrid improper ferroelectric mechanism recently proposed by Benedek and Fennie for these Ruddlesden-Popper compounds. However, in $Ca_3Mn_2O_7$ we find that there is a complex competition between lattice modes of different symmetry which leads to a phase coexistence over a large temperature range and the "symmetry trapping" of a soft mode. This trapping of the soft mode leads to a large uniaxial negative thermal expansion (NTE) reaching a maximum between 250 and 350 K (3.6×10^{-6} K^{-1}) representing the only sizable NTE reported for these and related perovskite materials to date. Our results suggest a systematic strategy for designing and searching for ceramics with large NTE coefficients.

DOI: 10.1103/PhysRevLett.114.035701 PACS numbers: 64.60.-i, 63.20.Ry, 65.40.De, 77.80.bg

A variety of physical phenomena are understood to give rise to ferroelectricity in the solid state, but the precise nature of the microscopic mechanisms is often unclear. The responsible physical phenomena include single ion effects such as lone pair and second-order Jahn-Teller ordering [1]. Ion size mismatch in the lattice may also lead to the off-center distortions of cations resulting in the development of ferroelectric polarization, and subtle polar distortions may be caused by magnetic, charge, and molecular-like ordering [2,3]. Whatever the origin of the microscopic mechanism, the responsible physical process causes an instability in the Γ point of the parent structure resulting in the ordering of a ferroelectric (polar) phonon mode.

The improper ferroelectric mechanism is where this polarization is only a secondary order parameter of the phase transition, a possibility first explored by Indenbom in 1960 [4]. This mechanism was first implemented to explain the ferroelectric phase transition in gadolinium molybdate [5,6], where it was believed that the spontaneous polarization was driven by an elastic (nonpolar) instability, and, shortly afterwards, Pytte [7] suggested that this elastic instability in gadolinium molybdate itself is coupled to a structural distortion with a nonzero propagation vector.

Because of the relatively simple structure of the perovskite and perovskite-related materials, classification and rationalization of their structural distortions have attracted a considerable amount of work over the past decades [8–11]. Recently, it has been shown that, in perovskite thin films, improper ferroelectricity may be induced via strain coupling of octahedral rotations between different perovskite heterostructure layers [12]. Benedek and Harris [13,14] developed this idea further proposing a novel mechanism where this improper ferroelectricity may be realized in the bulk structure. In this mechanism, instability of the polar phonon mode is driven by the condensation of two nonpolar lattice modes, neither of which are zone centered. This higher-order coupling of these two degrees of freedom with the polarization, coined "hybrid improper ferroelectricity," has been proposed to be responsible for the polar symmetry observed in the Ruddlesden-Popper (RP) $Ca_3Ti_2O_7$ and $Ca_3Mn_2O_7$ compounds. We present here to our knowledge the first experimental evidence corroborating this picture but show that a competing ground state structure in $Ca_3Mn_2O_7$ leads to "symmetry trapping" of a soft phonon mode resulting in large uniaxial negative thermal expansion (NTE).

The RP series $A_{n+1}B_nO_{3n+1}$, for favorable A and B cations, form a near-infinite homologous series of materials whose structure may be described as containing n slabs of the perovskite structure interspersed periodically with an AO rock salt layer along the c axis. Our Letter discusses the $n = 2$ family [Fig. 1(a)], $A = Ca^{2+}$, $B = Ti^{4+}$ and Mn^{4+}, but many other derivatives are known for A = Ca, Sr, La, B = Ti, Mn, V, Fe, Ru, and Ir. The family of these compounds exhibits many interesting physical phenomena including superconductivity, magnetoresistivity, and multiferroicity [15].

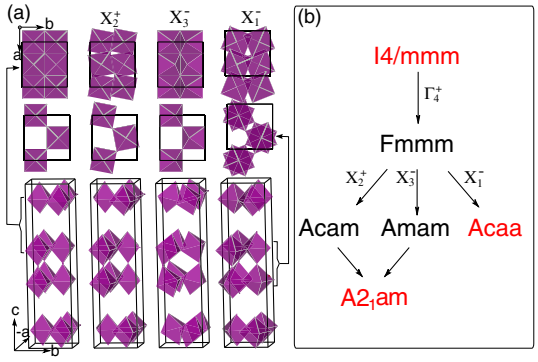

FIG. 1 (color online). (a) Rotating and tilting of the BO_6 octahedra under the various distortion modes of symmetry X_1^-, X_2^+, and X_3^- discussed in the Letter. (b) The relationship between the various symmetries of the high-temperature and low-temperature phases of $Ca_3Mn_2O_7$ and $Ca_3Ti_2O_7$, basis, and origin shift along with further details are given in Supplemental Material [16].

We have performed high-resolution diffraction to investigate the ferroelectric mechanisms in these materials. This comparative study between two family members, for neither of which single ion effects are expected to be important, allows us to exclusively probe the role of lattice-phonon coupling in the proposed ferroelectric mechanisms. Polycrystalline samples of $Ca_3Ti_2O_7$ and $Ca_3Mn_2O_7$ were prepared by standard solid-state synthesis methods at 1300–1500 °C. These samples were studied by high-resolution x-ray powder diffraction [$\lambda = 0.825630(1)$ Å] at I11, Diamond Light Source between 85 and 500 K and by medium-resolution neutron powder diffraction at INES, ISIS at 150 and 500 K. Rietveld analysis was performed on both samples across the whole temperature range by using the least squares refinement program Topas with the JEDIT interface [17]. Full details and fits are given in Supplemental Material [16]. The fits reveal that the samples are stoichiometric, and we do not observe the presence of substantial asymmetry in the diffraction profile and shift in peak positions reported previously [18–20], suggesting that our samples have a very low concentration of stacking faults and are highly crystalline. At 500 K, on first inspection, both samples index on the expected aristotypical symmetry for these Ruddlesden-Popper $n = 2$ compounds, $I4/mmm$ [Fig. 1(a), left]. However, weak additional reflections at $(h+\frac{1}{2}, k+\frac{1}{2}, l)$ were visible in both compounds, indicating that their symmetry must be lower than $I4/mmm$ even well above room temperature. These superstructure reflections index on the previously proposed $A2_1am$ supercell [20] [basis with respect to parent symmetry $= (1,-1,0),(-1,-1,0),(0,0,-1)$, origin $= (\frac{1}{4},\frac{1}{4},\frac{-1}{2})$]. Rietveld refinements at these temperatures yield good fits ($R_{WP} = 8.62$ and 12.30 for $Ca_3Mn_2O_7$ and $Ca_3Ti_2O_7$, respectively). The $A2_1am$ structure corresponds to the direct sum of the symmetry spaces spanned by $Acam$ and $Amam$ [see Fig. 1(a) and Supplemental Material [16] for full details] and is due to the simultaneous ordering of X_2^+ and X_3^- irreducible representations of the parent space group $I4/mmm$ under the ordering propagation vector $[\frac{1}{2},\frac{1}{2},0]$. As pointed out by Benedek [13], it is the simultaneous ordering of these two representations which broadly corresponds to a rotation of the BO_6 octahedra (X_2^+) and their tilting (X_3^-) along the c axis which sufficiently define the polar symmetry of the child space group without the need for explicit coupling of the zone-centered polar representation (Γ_5^-) which forms only a secondary order parameter of the phase transition in this case. Such a fortuitous ordering of these two primary order parameters is not expected by the Landau theory of second-order phases transitions, and a "hybrid" coupling between these two degrees of freedom to explain the phenomenology of the phase transition was invoked by Benedek *et al.*

To investigate the validity of such a hybrid order parameter, we have analyzed the atomic displacements in $Ca_3Ti_2O_7$ as refined in the Rietveld analysis in the temperature range 130–500 K in terms of symmetry-adapted distortion modes [21] which may be characterized by their ordering propagation vector, the irreducible representation to which they belong, the Wyckoff site in the parent symmetry on which they act, and their character with respect to that Wyckoff site symmetry. In total, the $A2_1am$ child structure has 19 internal degrees of freedom (plus the three lattice parameters). These are decomposed into four Γ_1^+, seven Γ_5^-, two X_2^+, and six X_3^- distortion modes (full details are given in Supplemental Material [16]). The evolution of all of these modes as a function of temperature for $Ca_3Ti_2O_7$ is given in Supplemental Material [16] and justifies, along with symmetry constraints, the fact that we focus on the X_2^+ rotation and X_3^- tilt associated with the oxygen distortions in the following discussion. We note also that the Γ_5^- distortions explicitly enter into the calculated polarization, and this order parameter is discussed later in the Letter. In order to demonstrate a hybrid coupling between the X_2^+ and X_3^- order parameters, Benedek [13] showed that the total internal energy (U) reaches a minimum for a structure involving distortions with both these characters. Here we demonstrate that by changing the temperature (and hence the balance of U with the free energy) both mode amplitudes $Q_{X_2^+}$ and $Q_{X_3^-}$ respond in proportion to one another (Fig. 2), indicating that the free energy of the system is stabilized by their coupling in $Ca_3Ti_2O_7$. We do not, however, observe a phase transition to $I4/mmm$ even up to 1150 K, by which point the sample starts to decompose (see Supplemental Material [16]), and hence the second-order nature of the hybrid order parameter proposed in Ref. [13] is still in question.

In Fig. 3, we plot the evolution of the ferroelectric polarization of $Ca_3Ti_2O_7$ as a function of temperature calculated in the point charge approximation [22]. The calculated polarization is shown to evolve continuously

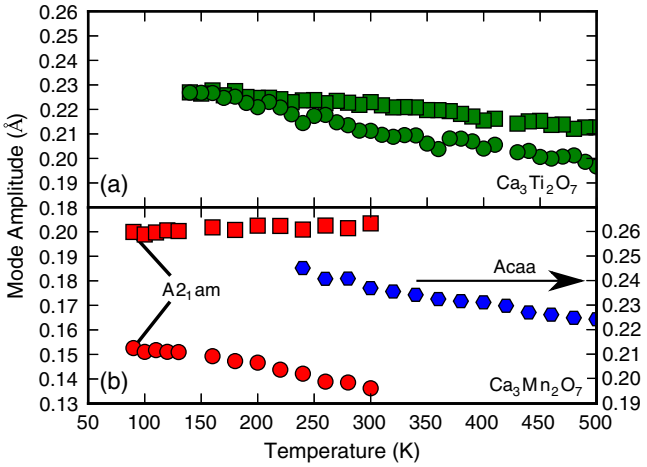

FIG. 2 (color online). Evolution of the distortion modes of symmetry X_1^-, X_2^+, and X_3^- (hexagonal, square, and circular symbols, respectively) with temperature. (a) Evolution of modes in the $A2_1am$ phase of $Ca_3Ti_2O_7$; (b) evolution of the modes X_2^+ and X_3^- in the low-temperature ($A2_1am$) phase and of the X_1^- mode in the high-temperature ($Acaa$) phase of $Ca_3Mn_2O_7$.

with temperature in proportion to $Q_{X_2^+}$ and $Q_{X_3^-}$. Our values calculated in this approximation are in good agreement with those reported in the literature that are derived for the ground state structure as optimized by density functional theory ($P = 20$ and $5\ \mu C\,cm^{-2}$ for $Ca_3Ti_2O_7$ and $Ca_3Mn_2O_7$, respectively) [13]. The strong correlation of the polarization with $Q_{X_2^+}$ and $Q_{X_3^-}$ as evident by comparing Figs. 2(a) and 3 [person R, -0.92 and -0.94 for $(Q_{X_2^+}, P)$ and $(Q_{X_3^-}, P)$, respectively] supports the hybrid improper ferroelectric mechanism in this material.

Although $Ca_3Mn_2O_7$ has been touted as a prototype system for this hybrid mechanism, we now show that the situation for this compound is somewhat different. $Ca_3Mn_2O_7$ is observed to have a phase coexistence at room temperature as previously reported [20], suggesting inconsistencies with a second-order phase transition of a hybrid order parameter. Furthermore, the high-temperature

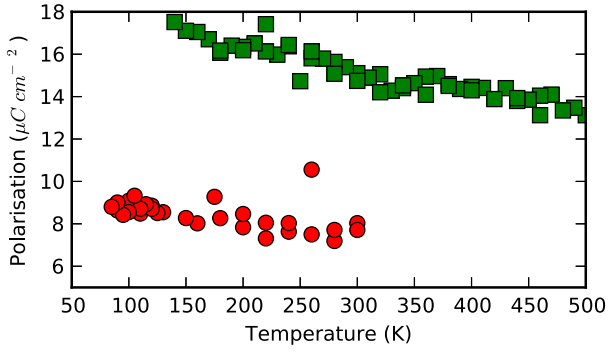

FIG. 3 (color online). Evolution of the polarization of $Ca_3Ti_2O_7$ (green squares) and $Ca_3Mn_2O_7$ (red circles, in the low-temperature $A2_1am$ phase only) as a function of temperature.

phase appears also to index on an $A2_1am$ cell but with lattice parameters that deviate substantially from the low-temperature phase (Rietveld refinement in the parent $I4/mmm$ space group gave a considerably worse fit of $R_{WP} = 10.71$ versus $R_{WP} = 8.62$ for $A2_1am$). The implied phase transition in this case would have no broken symmetry and offers no explanation to the origin of the unexpected phase coexistence. Reinvestigation of the high-temperature structure revealed that, although the $A2_1am$ model broadly captures the intensity of the superstructure peaks, it generates spurious intensity not observed in the diffraction pattern (see Supplemental Material [16]). We performed an exhaustive search of the isotropy subgroups of $I4/mmm$ compatible with the $[\frac{1}{2}\frac{1}{2}0]$ propagation vector. A model refined in the space group $Acaa$ provided the only good fit to the superstructure peaks ($R_{WP} = 8.10$; see Supplemental Material [16]). This model corresponds to an ordering of an X_1^- mode [Fig. 1(a)], a rotation of the BO_6 octahedra along the c axis out of phase within a perovskite slab. Such a mode is in competition with an X_2^+ in-phase rotation which clearly cannot coexist with the X_1^- mode within the same perovskite slab. Symmetry analysis [Fig. 1(b)] does indeed reveal that neither $Acam$, $Amam$, or $A2_1am$ form subgroups of $Acaa$ and the lowest symmetry space group of which all these symmetry spaces are a subgroup is $Fmmm$. $Fmmm$ has the equivalent Γ_1^+ distortions as present in $I4/mmm$ but with an additional orthorhombic lattice strain mode (Γ_4^+). There is hence no direct pathway along which the $Acaa$ phase may distort to reach its low-temperature form of $A2_1am$. We note that in the low-temperature ferroelectric phase of $Ca_3Mn_2O_7$ there is no strong evidence for a coupling between X_2^+ and X_3^- [Fig. 2(b)] and the polarization (Fig. 3). A possible explanation for this is that the discontinuous nature of the phase transition leads to a loss of long-range coherence between these degrees of freedom.

To investigate this abnormality in the phenomenology of the symmetry relationships, we have performed a multi-phase Rietveld refinement fit of the two phases across the entire temperature range. We must emphasize that the high resolution we achieved in our synchrotron powder diffraction experiments ($\Delta d/d = 10^{-3}$–10^{-4} Å) is essential for this work. Figure 4(a) shows the evolution of the phase fraction as a function of temperature on cooling and warming from 500 to 85 to 460 K. We observed a phase coexistence over a very large temperature range (200–320 K) and a substantial hysteresis (≈70 K) on warming and cooling. The hysteresis is consistent with our symmetry analysis, which indicates that this cannot be considered as a second-order phase transition and there is an activation barrier that must be overcome to nucleate an $Acaa$ from an $A2_1am$ domain, and vice versa. Phase coexistence along with hysteresis is expected for a first-order phase transition [23], although over such a broad temperature range it is unusual.

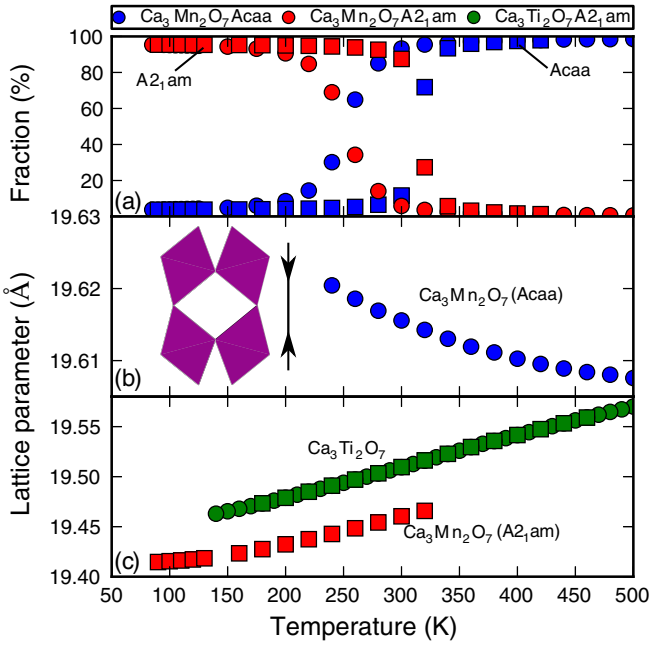

FIG. 4 (color online). (a) Evolution of the phase fraction in $Ca_3Mn_2O_7$ as a function of temperature. (b) Negative thermal expansion along the c-axis of $Ca_3Mn_2O_7$ at high temperatures consistent with a soft mode mechanism (shown in inset) (c) positive thermal expansion of the c-axis in $Ca_3Ti_2O_7$ and in $Ca_3Mn_2O_7$. Circle and square symbols represent data collected on cooling and warming respectively, and all e.s.u. are small than the size of the symbols.

To investigate this further, in Figs. 4(b) and 4(c), we plot the c lattice parameters of the two refined phases of $Ca_3Mn_2O_7$ over the temperature ranges for which they are observed. What becomes evident is that the two phases exhibit markedly different behavior. The *Acaa* phase exhibits a pronounced uniaxial NTE along the c axis with rising gradient down to the point at which the phase vanishes beyond the signal to noise resolution of our experiment. The coexisting low-temperature $A2_1am$ phase, on the other hand, adopts the expected positive thermal expansion (PTE) with linear gradient from the point at which it starts to crystallize out. This phase has the same PTE behavior as $Ca_3Ti_2O_7$ exhibits across the entire temperature range [Fig. 4(c)], and all three phases have a similar volume contraction following the expected PTE (see Supplemental Material [16]).

The reported cases of NTE in the literature fall broadly into two categories being due to either electronic ordering phenomena such as charge transfer or transverse vibrations of (quasi)rigid unit modes (RUMs) [24]. Although to date sizable NTE has been reported only in perovskitelike materials where electronic effects play a role (e.g., $BiNiO_3$ [25]), we can discount such mechanisms in the current case (Mn^{4+}, $t_{2g}^{\uparrow\uparrow\uparrow}$, no single ion effects expected) and so must conclude that RUMs are responsible for the observation. The quasirigid units in our system are the BO_6 octahedra, and, although these are commonly observed to give rise to NTE in network, cage, and framework structure [26], in the perovskite oxides it has been observed in only a few cases (e.g., uniaxial NTE in WO_3 [27]), where it leads to near-zero thermal expansion.

The thermal excitation of such RUMs can lead to a substantial lattice contraction as demonstrated in the inset in Fig. 4(b) for a RUM of X_3^- character in the limit where the phonon population for any longitudinal B-O stretching vibrations is significantly smaller than the population of the transverse phonon RUMs. The X_3^- RUM may only contribute to NTE in the *Acaa* phase where it has not "frozen out" as has occurred in the $A2_1am$ phase where only PTE is observed. The observed uniaxial NTE coefficient is -3.6×10^{-6} K^{-1} over the temperature range 250–350 K comparing favorably with the significantly more flexible framework ZrW_2O_8 structure (isotropic NTE of -9.0×10^{-6} K^{-1}) which represents the eponymous example of NTE in the solid state [28]. It seems probable in the present case of $Ca_3Mn_2O_7$ that it is only due to the symmetry trapping of the X_3^- mode by the high-temperature *Acaa* phase that this material is able to exhibit a genuine signature of NTE, and without this mechanism normal PTE would be observed as in $Ca_3Ti_2O_7$. The comparison of the symmetry of the low-temperature and high-temperature phases of $Ca_3Mn_2O_7$ has allowed us to identify the character of this soft phonon mode (X_3^-), a situation possible in most other NTE materials only after extensive theoretical work. We note that our observations here of NTE in the nonpolar phase of $Ca_3Mn_2O_7$ are completely unrelated to the observation of strain coupling in the polar phase of the improper ferroelectric artificial superlattice perovskite [12] which results in an increase in tetragonality (c/a) at low temperature and is unrelated to NTE.

Our symmetry trapping mechanism we propose here is completely general, and a search criteria below for the discovery of new NTE materials is as follows. First, any parent structure which has two closely competing phases of symmetry A and B, where A is stable at high temperature and B is stable at low temperature but they do not follow a subgroup relationship, should be considered as a candidate. Second, systems where distortion modes belonging to irreducible representations of the parent symmetry present in B but absent in A with a transverse displacive or RUM character should be considered. Third, since the most successful candidates of NTE will be ones where the phase transition to symmetry B is suppressed to very low temperatures (and may be experimentally unreported), families of compounds who are isostructural with respect to their parent symmetries but depending on their exact chemical composition exhibit either ground states of symmetry A or B should be considered. Of course, parent structures may be relaxed via electronic structure calculations in order to identify compounds likely to exhibit symmetries of both A and B—or phonon density of states calculated to identify

possible competing instabilities; however, our method presented here has its strength in that it relies only on symmetry analysis and database mining—making a large-scale survey of all known crystal structures computationally realistic. We note that the large number of perovskite-related materials will be a promising area to start this search.

The difference in behavior of $Ca_3Mn_2O_7$ and $Ca_3Ti_2O_7$, which have very closely related lattice constants, is interesting and may be related to the fact that the lattices are over- or understrained, respectively, on account of the differing ionic radii of the B-site cations ($Mn/Ti = 0.88$) [29]. The structural simplicity of the corner-sharing network of octahedra present in this perovskite-related compound will make the theoretical exploration of NTE in these materials particularly appealing, and we predict that doping the large family of Ruddlesden-Popper compounds to control this strain will lead to the realization of many new NTE materials utilizing our symmetry trapping mechanism.

In summary, while our results support the hybrid improper ferroelectric mechanisms in $Ca_3Ti_2O_7$, for $Ca_3Mn_2O_7$ the situation is shown to be far more complex where a competing soft mode "trapping" mechanism leads to a large uniaxial NTE in the high-temperature nonpolar phase. We predict that engineering materials to control the behavior of soft modes via symmetry trapping in these and the host of other related compounds (Ruddlesden-Popper $n = 1$–∞, Aurivillius phases, and high-T_c superconducting cuprates) will enable the exploration of rich phase diagrams for materials exhibiting NTE.

We acknowledge Diamond Light Source (Proposal No. EE9677) and the STFC and the Italian CNR (Cooperation Agreement No. 06/20018) for awarding us time on I11 and INES, respectively. The work at Rutgers University was supported by the DOE under Grant No. DE-FG02-07ER46382, and the work at Postech has been supported by the Max Planck POSTECH/KOREA Research Initiative Program [Grant No. 2011-0031558] through NRF of Korea funded by MEST. MSS would like to acknowledge the Royal Commission for the Exhibition of 1851 for a fellowship.

*mark.senn@chem.ox.ac.uk

[1] C. Ederer and N. A. Spaldin, Nat. Mater. **3**, 849 (2004).
[2] K. Yamauchi and P. Barone, J. Phys. Condens. Matter **26**, 103201 (2014).
[3] C. N. R. Rao, A. Sundaresan, and R. Saha, J. Phys. Chem. Lett. **3**, 2237 (2012).
[4] V. Indenbom, Kristallografiya **5**, 115 (1960).
[5] L. Cross, A. Fouskova, and S. Cummins, Phys. Rev. Lett. **21**, 812 (1968).
[6] A. P. Levanyuk and D. G. Sannikov, Sov. Phys. Usp. **17**, 199 (1974).
[7] E. Pytte, Solid State Commun. **8**, 2101 (1970).
[8] A. M. Glazer, Acta Crystallogr. Sect. B **28**, 3384 (1972).
[9] D. Hatch and H. Stokes, Phys. Rev. B **35**, 8509 (1987).
[10] K. S. Aleksandrov and J. Bartolome, J. Phys. Condens. Matter **6**, 8219 (1994).
[11] H. T. Stokes, E. H. Kisi, D. M. Hatch, and C. J. Howard, Acta Crystallogr. Sect. B **58**, 934 (2002).
[12] E. Bousquet, M. Dawber, N. Stucki, C. Lichtensteiger, P. Hermet, S. Gariglio, J.-M. Triscone, and P. Ghosez, Nature (London) **452**, 732 (2008).
[13] N. A. Benedek and C. J. Fennie, Phys. Rev. Lett. **106**, 107204 (2011).
[14] A. B. Harris, Phys. Rev. B **84**, 064116 (2011).
[15] R. H. Mitchell, *Perovskites Modern and Ancient* (Almaz Press, Thunder Bay, Ontario, 2002), p. 143.
[16] See Supplemental Material at http://link.aps.org/supplemental/10.1103/PhysRevLett.114.035701 for further details of symmetry analysis, Rietveld refinements and the temperature evolution of refined parameters for $Ca_3Ti_2O_7$ and $Ca_3Mn_2O_7$.
[17] J. S. O. Evans, Mater. Sci. Forum **651**, 1 (2010).
[18] M. M. Elcombe, E. H. Kisi, K. D. Hawkins, T. J. White, P. Goodman, and S. Matheson, Acta Crystallogr. Sect. B **47**, 305 (1991).
[19] N. Guiblin, D. Grebille, H. Leligny, and C. Martin, Acta Crystallogr. Sect. C **58**, i3 (2002).
[20] M. V. Lobanov, M. Greenblatt, E. A. N. Caspi, J. D. Jorgensen, D. V. Sheptyakov, B. H. Toby, C. E. Botez, and P. W. Stephens, J. Phys. Condens. Matter **16**, 5339 (2004).
[21] B. J. Campbell, H. T. Stokes, D. E. Tanner, and D. M. Hatch, J. Appl. Crystallogr. **39**, 607 (2006).
[22] N. A. Spaldin, J. Solid State Chem. **195**, 2 (2012).
[23] K. Binder, Rep. Prog. Phys. **50**, 783 (1987).
[24] K. D. Hammonds, M. T. Dove, A. P. Giddy, V. Heine, and B. Winkler, Am. Mineral. **81**, 1057 (1996).
[25] M. Azuma, W.-T. Chen, H. Seki, M. Czapski, S. Olga, K. Oka, M. Mizumaki, T. Watanuki, N. Ishimatsu, N. Kawamura, S. Ishiwata, M. G. Tucker, Y. Shimakawa, and J. P. Attfield, Nat. Commun. **2**, 347 (2011).
[26] C. Lind, Materials **5**, 1125 (2012).
[27] C. Rosen, E. Banks, and B. Post, Acta Crystallogr. **9**, 475 (1956).
[28] J. S. O. Evans, T. A. Mary, T. Vogt, M. A. Subramanian, and A. W. Sleight, Chem. Mater. **8**, 2809 (1996).
[29] H. Shaked, J. Jorgensen, O. Chmaissem, S. Ikeda, and Y. Maeno, J. Solid State Chem. **154**, 361 (2000).